

STUDIES ON ION SCATTERING AND SPUTTERING PROCESSES IN ION
BEAM SPUTTER-DEPOSITION OF HIGH T_c SUPERCONDUCTING FILMS:
THE OPTIMIZATION OF DEPOSITION PARAMETERS

Received by OSTI

MAY 09 1990

M. S. Ameen, O. Auciello¹, and A. I. Kingon
N. C. State University, Department of Materials Science and Engineering, Raleigh, NC
27695-7907

1. Also Microelectronics Center of North Carolina, Research Triangle Park, NC
27709-2889

A. R. Krauss
Argonne National Laboratory, Chemistry Division, Argonne, IL 36409

M. A. Ray
Microelectronics Center of North Carolina, Research Triangle Park, NC 27709-2889

ABSTRACT

Ion beam sputter-deposition is one of the techniques used for synthesizing high T_c superconducting films in laboratory experiments. However, the scaling-up of this method for technological applications, such as in microelectronics, will require a better understanding of basic phenomena occurring during the deposition process. First results are presented here from experimental and computer simulation studies on ion scattering and sputtering processes. It is demonstrated that scattering of neutralized ions from the targets can result in undesirable erosion of, and inert gas incorporation in, the growing films, depending on the ion/target atom mass ratio and ion beam angle of incidence/target/substrate geometry. The studies indicate that sputtering by Kr^+ or Xe^+ ions is preferable to the most commonly used Ar^+ ions, since the undesirable phenomena mentioned above are minimized for the first two ions. These results are used to determine optimum sputter deposition geometry and ion beam parameters for growing high T_c films.

INTRODUCTION

Ion beam sputter-deposition is one of the techniques currently used at the laboratory scale for synthesizing high T_c superconducting thin films.^{1,2} Most films hitherto deposited by this technique have been produced by sputtering multicomponent superconductor oxide targets with high intensity ion beams.^{1,2} Control of film stoichiometry is difficult using these targets, due in part to processes such as preferential sputtering and varying sticking coefficients of the sputtered species on the substrate. To control these effects, researchers have developed ion beam deposition systems featuring single element or oxide targets configurations, either with multiple ion beams³ to sputter each elemental target, or rotating multiple target holder and a single ion beam⁴ directed at a fixed position to sequentially sputter each target. Little information is available, however, on basic ion scattering and sputtering processes occurring in ion-target interactions during film deposition, and their influence on film characteristics at the ion beam energies and fluxes that are typically used in these systems.

In this paper we report selected results from an in depth study of sputtering and scattering phenomena occurring when using low energy (1-2 keV) ion beams on target materials used to produce superconducting films. In order to produce high quality films of these materials, a precise understanding of the ion-surface interactions and

MASTER
So

DISCLAIMER

This report was prepared as an account of work sponsored by an agency of the United States Government. Neither the United States Government nor any agency thereof, nor any of their employees, makes any warranty, express or implied, or assumes any legal liability or responsibility for the accuracy, completeness, or usefulness of any information, apparatus, product, or process disclosed, or represents that its use would not infringe privately owned rights. Reference herein to any specific commercial product, process, or service by trade name, trademark, manufacturer, or otherwise does not necessarily constitute or imply its endorsement, recommendation, or favoring by the United States Government or any agency thereof. The views and opinions of authors expressed herein do not necessarily state or reflect those of the United States Government or any agency thereof.

DISCLAIMER

Portions of this document may be illegible in electronic image products. Images are produced from the best available original document.

related film growth mechanisms is necessary. We have examined the sputter yield of various elemental and oxide precursor materials, the deposition rate of these materials for various ion beam parameters, and the amount of gas trapping occurring in the film during deposition. Results are compared to calculations done with a modified TRIM code⁵ in order to determine dominant effects and optimize deposition parameters.

EXPERIMENTAL METHODS AND RESULTS

Experiments were performed in a turbopumped stainless steel chamber with a base pressure of 1×10^{-7} torr. The ion beam was produced by a Kaufman-type ion source with collimated extracting grids. The ion source was typically operated at 1.4 KeV and 25 mA, except where noted. High purity Ar, Kr, or Xe gas was introduced via a mass flow controller at 2.00 sccm, resulting in an operating chamber pressure of $1.0 - 5.0 \times 10^{-4}$ torr with the ion beam off. High purity metallic Cu, Y, and Ba targets were used for all the experiments, and they were sputter-cleaned before acquiring data on sputtering and scattering processes.

The measurements were made using the deposition geometry shown in Figure 1. Films were deposited onto substrates at the 30° , 60° , and 90° positions indicated in Figure 1, with the sputter-ion beam impacting the target at either 45° or near normal incidence. Films were deposited on glass slides or, in the case of barium, on silicon. Deposition rates were determined either by profilometry of the deposited films or by positioning a quartz crystal resonator in the desired position. A comparison of the two techniques yielded identical results for Cu films.

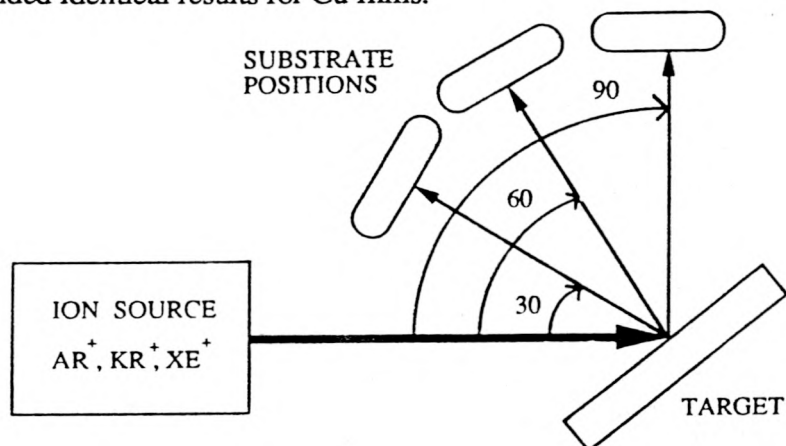


Fig. 1. System geometry used for measuring deposition rates and for determining gas trapping. The sketch above shows the ion beam impacting at 45° to the target surface normal.

Studies of gas trapping in films were performed by secondary ion mass spectrometry (SIMS) using a Cameca instrument. Relative concentrations of Ar, Kr, and Xe gases were obtained as a function of depth into the film.

Figure 2 shows the relative amount of sputtering gas incorporated into Cu, Y, and Ba films at the $30^\circ/60^\circ/90^\circ$ substrate positions relative to the incoming ion beam. The beam-target angle was 45° with respect to the target normal, as shown in Figure 1. Films were deposited at all positions ($30^\circ/60^\circ/90^\circ$) simultaneously to minimize run-to-run deviations.

Inspection of the data in Figure 2 shows that the amount of Ar trapped in the films decrease from the 90° to 30° substrate positions. The quantification of SIMS data is, however, difficult, due in part to large matrix effects which may alter the relative

intensity of the signals measured. Therefore, in this paper, we consider only the relative trends observed, and postpone a more quantitative study for when we obtain standard samples by Ar⁺ ion implantation in specially deposited films. The Ar and Ca peaks are not resolvable in the system used for these analyses. Therefore, the CsAr⁺ (mass 173) peak was monitored, and energy spectra were taken at various stages during the profiling to assure that a sharp peak, characteristic of the easily dissociable CsAr⁺ molecule, was observed, opposite to a long tailed peak, which would appear if a CsCa⁺ molecule was being produced. Details of this analysis will be published elsewhere.

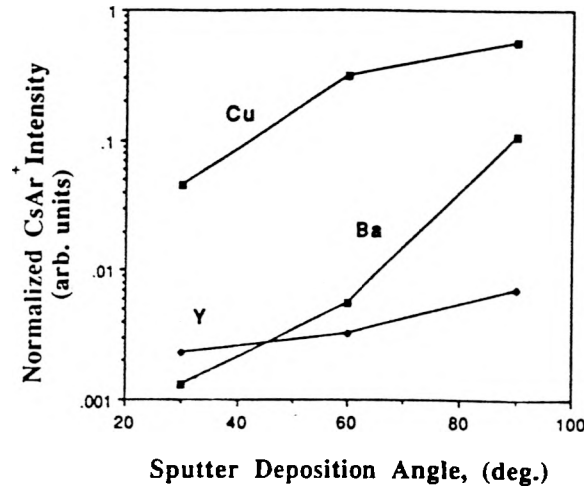


Fig. 2. SIMS data showing relative amount of Ar gas incorporated into Cu, Y, and Ba films deposited with a 1.4 keV ion beam at 25 mA. Steady-state SIMS count levels were used. The trapping of Xe is not plotted, as no signals above background level was detected within the sensitivity of the CAMECA instrument used. This indicates that incorporation of Xe in the films is negligible. Further work is necessary to determine Kr incorporation into films.

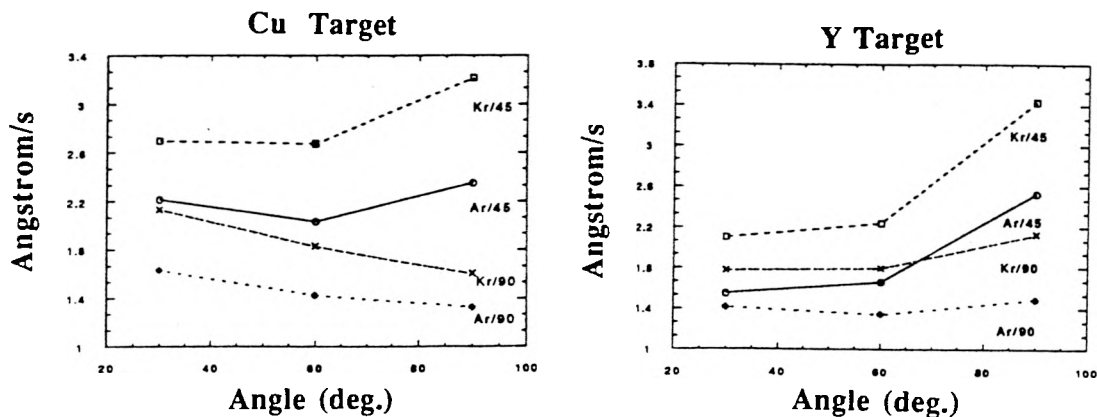


Fig. 3. Deposition rate of Cu and Y films at 30°, 60°, and 90° substrate positions relative to the ion beam (see Fig. 1) for both 45° and normal ion beam incidence (1.4 keV, 25 mA).

Figure 3 shows the deposition rate of Cu and Y, for both 45° and normal ion beam incidence on the target, as a function of substrate position relative to the incoming ion beam. The data indicates that there is a larger net deposition rate, for 45° ion beam angle of incidence, in the forward (specular) sputtered flux direction (90° position in Figure 1). The deposition rate is greater for the higher mass ion beam (Kr), as expected from sputtering theory⁶ and experiments.⁷ The results in Figure 2 show that a minimum occurs in the deposition rate of Cu at the 60° position for 45° ion beam incidence (a minimum was also observed for the Ba deposition, although it was less pronounced). On the other hand, Figure 3 indicates that the gas trapping, which is correlated with the scattered flux from the target, is a continuously increasing function of the substrate position. This suggests that measurements of the sputtered and scattered fluxes at each position will be necessary to determine their interdependence and therefore their influence in controlling deposition rates. The effects of ion scattering on the deposition process, in view of the data presently available, are discussed in detail below.

COMPUTER MODELLING RESULTS

We have performed computer simulations of the sputtering and scattering processes to establish qualitative correlations with the experimental results. The TRIM code⁵ has been used to generate the data presented in Figures 4-6.

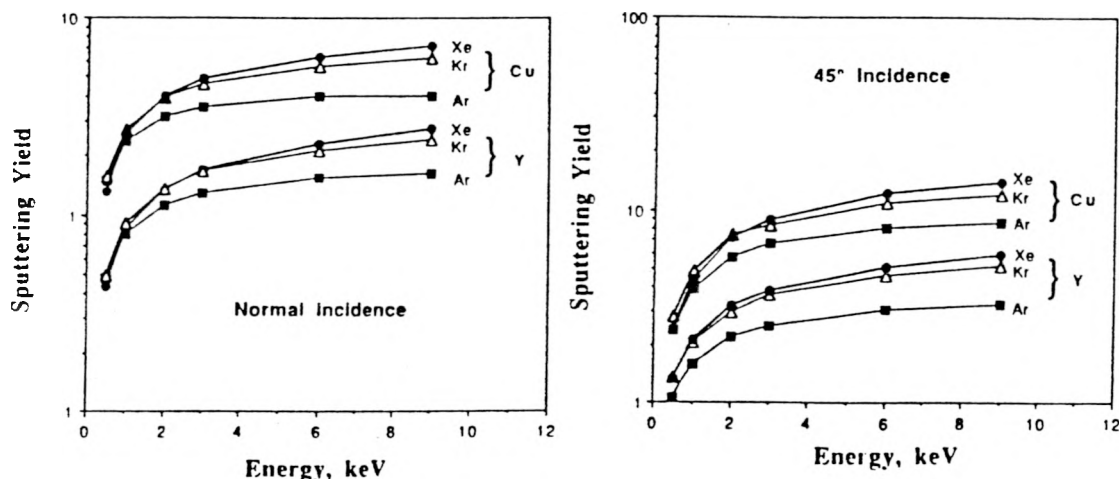


Fig. 4. Sputtering Yields (Y_s) vs. beam energy for Ar^+ , Kr^+ , and Xe^+ ion bombardment of Cu, and Y for normal and 45° ion beam incidence with respect to the target surface normal.

Figures 4 and 5 show the results of TRIM calculations for the sputtering yield of Cu, Y and Ba as a function of the ion beam energy for both normal and 45° beam incidence. The data confirms that the well known dependence of sputter yield on beam energy extends to the low keV range. Also observed is the dependence of Y_s on ion and target mass and angle of incidence. However, the sputtering yield for Kr is seen to be closer to that for Xe even though the mass of Kr (80 amu) is nearer to Ar (40 amu) than to Xe (131 amu). This indicates that the sputtering yield will eventually increase very little for these target materials as the bombarding ion mass increases, resulting in only a small advantage when increasing the mass of bombarding ions from Kr to Xe. Practically,

the cost of Xe may be a limiting factor, especially when considering scaling the processing up for manufacturing purposes.

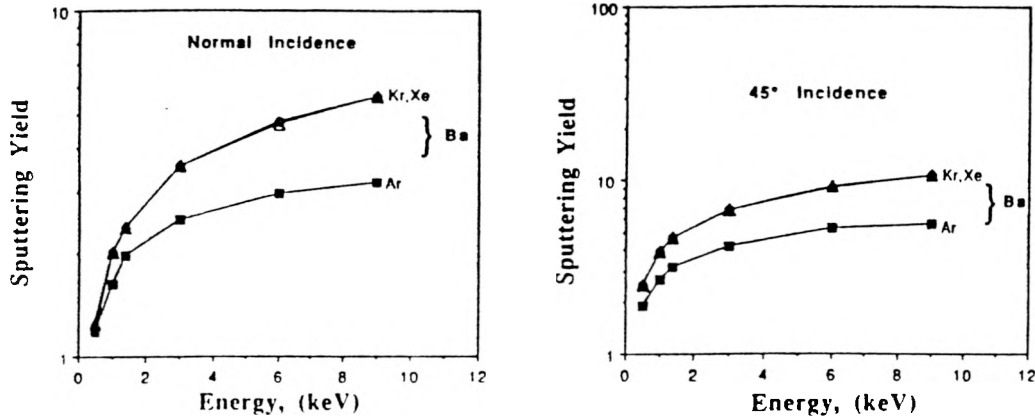


Fig. 5. Sputtering Yields (Y_s) vs. beam energy for Ar^+ , Kr^+ , and Xe^+ ion bombardment of Ba at normal and 45° ion beam incidence with respect to the target surface normal.

The sputtering yield of Cu is larger than the one corresponding to Y for both normal and 45° beam incidence. This result agrees with the data shown in Figure 3, and with previously reported measurements in these systems. The model predicts that the sputtering yield for 45° incidence is larger than for 90° for both Cu and Y. The data in Figure 3 confirms this trend, but the magnitude of the differences is much larger than predicted by the model. This discrepancy may be explained by taking into account the fact that the TRIM code⁵ counts all species ejected from the surface independent of the angle of ejection. The quartz crystal resonator used to measure the data in Figure 3 subtends only a small portion of the total ejected flux. Since this distribution is quite different for 45° and 90° incidences, the results are not surprising.

Calculations for the number of neutralized ions scattered from the target, as a function of the energy of the scattered species, are shown in Figures 6 and 7 for Cu and Ba respectively (results for Y are similar to those for Cu and will be discussed in a forthcoming more comprehensive paper). The model predicts a significant percentage of high energy (initial beam energy 1.4 keV) Ar species scattered from both Cu and Ba, while the number of scattered Kr and Xe are less. This result is to be expected based on the masses of the incident ions and target atoms. The model also predicts a lower high energy tail for Kr and Xe gases on both Y and Ba. These scattered energetic species can produce erosion of the growing films and be incorporated into them, which can affect their stoichiometry, microstructure and quality.

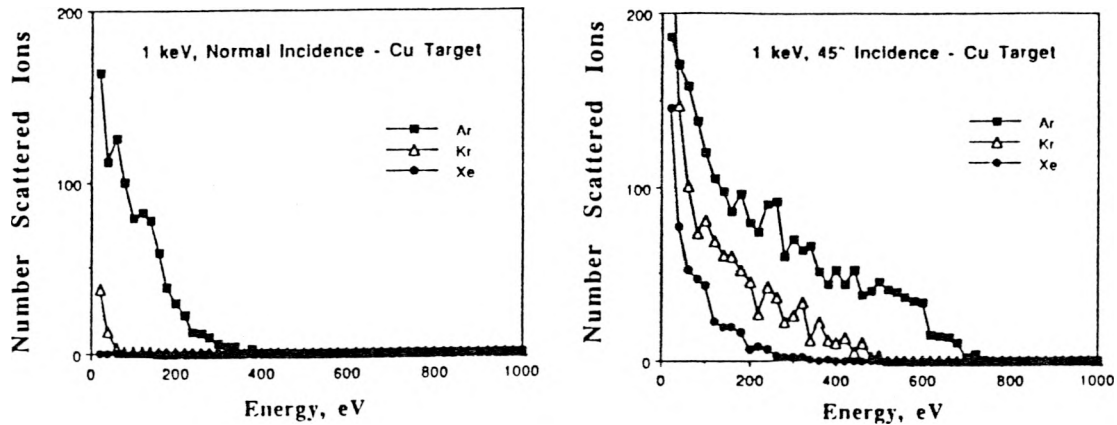


Fig. 6. Number of neutralized scattered ions vs. energy of the scattered species for Ar^+ , Kr^+ , and Xe^+ ion bombardment of Cu for normal and 45° ion beam angle of incidence on the target.

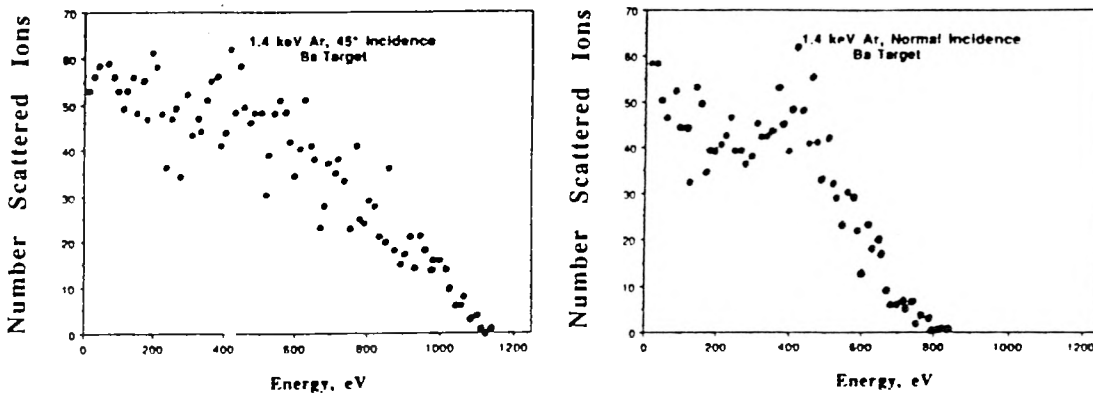


Fig. 7. Number of neutralized scattered ions vs. energy of the scattered species for Ar^+ ion bombardment of Ba for normal and 45° ion beam angle of incidence on the target.

The effects of ion scattering were first inferred from experimental results obtained while attempting to deposit Ba films using an Ar^+ ion beam incident at 45° onto a Ba target. In those experiments, it was observed that a much thinner film than expected for the particular deposition conditions was produced, concurrently with an erosion of the gold film contact of the quartz crystal monitor used to measure the film deposition rate and thickness. An analysis of the physics of the collision between Ar^+ ions (40 amu) and the much heavier Ba atoms (137 amu) indicated that the mass ratio was unfavorable for effective energy transfer from the ions to the atoms to initiate the collision cascades in the solid, which are necessary for an effective sputtering processes. Figure 6 shows the TRIM calculations of the energy of Ar^+ ions scattered from Ba for normal and 45° ion beam incidence. Comparison of the data in Figures 6

and 7 reveals that a much larger number of neutralized ions with relative high energies are scattered from Ba than from Cu. The analysis of the experimental and computer simulation data, within the present quantitative limitations, suggests that there is a competition between film erosion and gas trapping processes. For example, the comparison between Figures 2, 6, and 7 reveals that although there are more energetic scattered species from Ba than from Cu, there is more Ar gas trapped in the Cu than in the Ba film. This could be explained, at least qualitatively, by considering the following information obtained in our experiments: (a) the sputtering yield of Cu is higher than for Ba, which would result in a higher deposition rate for the first, provided the sticking coefficients for Cu and Ba, on the used substrates, are similar; (b) the erosion of the growing film is higher for Ba than for Cu, which could result in a more effective elimination of trapped Ar from the film, due to a resputtering process. Obviously, further work is necessary to quantify the qualitative analysis presented above; particularly, experiments including the production of standard films with a known quantity of implanted Ar at the same energies involved in the present experiments.

The information generated by the computer simulations can be used to gain qualitative insights regarding the sputtering and gas incorporation data, which indicate that the film deposition process involves a collection of interdependent phenomena simultaneously occurring at the substrate surface. This interdependence of competing phenomena certainly will influence the stoichiometry, microstructure and quality of the films. In relation to the previous statement, other works now appearing in the literature indicate that the scattering phenomena discussed in this paper may be generally involved in ion beam sputter-deposition of other materials, an example being ion beam reactive sputter-deposition of NbN films.⁸

The sputtering rate is a strong function of beam energy, ion and target mass, and ion beam angle of incidence, the highest rate being produced by using the largest ion mass at oblique incidence. However, other processes such as ion scattering become significant at oblique incidence. The effects of ion scattering are seen in both the increase in gas trapping as a function of angle and in a slightly depressed sputter rate at the 60° position (Figure 3) for Cu, Y, and Ba species. Also, the energy of the neutralized scattered ions, which increases for decreasing ion mass, causes a higher rate of resputtering and gas incorporation.

The deposition rate of Cu at the 60° substrate position may be explained in terms of these competing process occurring at the substrate. At this position, for this particular ion energy and ion and target masses, a balance of film resputtering due to energetic species bombardment and deposition is taking place. The amount of sputtered species increases significantly towards the ion beam specular reflection direction (90° substrate position in Figure 1) resulting in a net increased deposition (and increased gas incorporation). From this information, we expect that the sputtering of species will increase faster than the scattering of ions for directions closer to the specular reflection position at 90°. Future experiments, involving the measurement of the sputtered and ion scattered fluxes with a calibrated quadrupole in line of view to the target, may help in obtaining more quantitative data.

CONCLUSIONS

Following the analysis presented above, we can draw some conclusions about the optimum system geometry and ion beam parameters necessary to deposit high quality films by minimizing gas trapping and possible film damage by energetic neutralized scattered ions bombardment. The sputtering yield vs. ion energy data indicates that the highest yields are obtained for 45° ion beam incidence using Xe⁺ ions. However, the difference between the sputtering yields for Xe⁺ and Kr⁺ ions may

not be as substantial as to offset the high cost of the Xe gas. Sputtering with Ar gas results in higher energy neutralized scattered ions from the target surface, especially as the mass of the target atom increases. This results in film resputtering and gas incorporation. The scattering process can be reduced by depositing at the 30° substrate position with the beam impacting normal to the target, at a cost of deposition rate. The best compromise may be obtained by using Kr⁺ ions, which yields lower energy scattering and less tendency for trapping than Ar⁺ ions, for 45° ion beam incidence angle to maximize deposition rate. For heavier atomic mass unit target materials, a substrate position nearer 60° may be desirable to minimize any potential ion scattering. Further work will be necessary to quantify the data presented here, and is warranted, considering the impact that these studies may have in optimizing the parameters for the deposition of high quality superconducting films by ion beam sputter-deposition.

ACKNOWLEDGMENTS

This work was performed with support of the Defense Advanced Research Projects Agency (N-00014-88-K-0525). Partial support was also obtained from the Office of Naval Research (N-00014-88-K-0526), the National Science Foundation (DMR-88-07367), and the Department of Energy (Basic Energy Sciences W-31-109-ENG-38 and DEFG05-88ER-45359). The authors would like to acknowledge the partial technical support of graduate students Tom Graettinger, Clifford Soble, and Y.L. Liu.

REFERENCES

1. J.M.E. Harper, R.J.Colton, and F.C. Feldman (Eds.), Amer. Inst. Phys. Conf. Proc. No. 165 (1988).
2. G. Margaritondo, R. Joynt, and M. Onellion (Eds.), Amer. Inst. Phys. Conf. Proc. No. 182(1989).
3. S. Michel, J. H. James, B. Dwir, M. Affronte, B. Kellett, and D. Pavuna, "The Preparation of YBCO Thin Films by a Four Ion Beam Co-deposition System." Private communication (1989).
4. A.I. Kingon, O. Auciello, M.S. Ameen, S.H. Rou, and A.R. Krauss, Appl. Phys. Lett. 55 (1989) 301.
5. J.P. Biersack and W. Eckstein, Appl. Phys. A34 (1984) 73.
6. P. Sigmund, in "Sputtering by Particle Bombardment 1", R. Behrisch (Ed.), Springer-Verlag (1981) pp 9.
7. H.H. Andersen and H.L. Bay, in "Sputtering by Particle Bombardment 1", R. Behrisch (Ed.), Springer-Verlag (1981) pp 145.
8. D.J. Lichtenwalner, A.C. Anderson, and D.A. Rudman, these proceedings.

DISCLAIMER

This report was prepared as an account of work sponsored by an agency of the United States Government. Neither the United States Government nor any agency thereof, nor any of their employees, makes any warranty, express or implied, or assumes any legal liability or responsibility for the accuracy, completeness, or usefulness of any information, apparatus, product, or process disclosed, or represents that its use would not infringe privately owned rights. Reference herein to any specific commercial product, process, or service by trade name, trademark, manufacturer, or otherwise does not necessarily constitute or imply its endorsement, recommendation, or favoring by the United States Government or any agency thereof. The views and opinions of authors expressed herein do not necessarily state or reflect those of the United States Government or any agency thereof.